International Journal of Emerging Engineering Research and Technology
Volume 5, Issue 4, 2017, PP 26-35
ISSN 2349-4395 (Print) & ISSN 2349-4409 (Online)

Load Carrying Capacity of Clay Brick Masonry Wall Encased by Ferrocement

Wail N. Al-Rifaie[1] and Khaled Mohammad[2]

[1]*Professor of Civil Engineering, Philadelphia University, Amman-Jordan*
[2]*Research Scholar, University of Technology, Baghdad-Iraq*

***Corresponding Author:** Wail N. Al-Rifaie, Professor of Civil Engineering, Philadelphia University, Amman - Jordan.*

***Received Date:** 13-07-2017* ***Accepted Date:** 20-07-2017* ***Published Date:**31-07-2017*

ABSTRACT

The main aim of this study is to investigate the behaviour and ultimate strength of ferrocement-clay brick composite walls under axially compressive loads. Three ferrocement-brick composite walls were constructed and tested. In addition, one clay brick wall was built and coated with cement mortar in order to establish a basis for comparison. The main parameter considered was number of wire mesh layers. In addition, formulations of design guidelines for ferrocement-clay brick composites are carried out.

It is concluded that ferrocement-clay brick composite walls can be used as a compression element in housing components and for rise buildings. The addition of a number of wire mesh layers has small effect on the ultimate load.

Keywords: *ferrocement, composite, clay brick, masonry wall.*

INTRODUCTION

Brick work buildings belong to the oldest housing systems that mankind has invented. A masonry building characterized by walls that are arranged in arbitrary directions so that a very stiff structure is attained. Many building codes require in general, that masonry bearing walls should be at least 300mm thick for the top 10m of their height. Thickness should be increased 100mm for each successive 10m or fraction of this distance, measured down from the top of the wall.

Ferrocement-brick composite considered as a new type of construction consists of brick core and ferrocement casing, which is a form of cement: sand mortar reinforced with steel wire meshes with or without steel bars of small diameters called skeletal reinforcement. Ferrocement encased brick construction can considerably increase the load carrying capacity as well as moment resistance of brick masonry, leading to a decrease in the wall thickness and reducing the dead load on the foundation.

Singh et al [(1)] have tested masonry columns encased by ferrocement. They concluded that mean failure load was lowest for unplastered columns and highest for columns encased in ferrocement with sand: cement ratio of 2:1 and the failure load was double. Nayak and Jain[(2)] have conducted tests on specimens varying the thickness of masonry in which masonry acts as a filler material, thickness of ferrocement layer and type of wire mesh used to study the effect of these parameters on the strength and performance of the composite. It was concluded that the composite construction in masonry and ferrocement can be used with advantage in various applications. Al-Rifaie and Mohammad [(3)] tested 12 ferrocement-brick masonry composite columns up to failure. It was concluded that the failure loads of the composite increased up to three times of plain masonry columns and the failure is ductile.

Abid A. Shah [( )] in 2011 had conducted an experimental program on columns 221x221x784 mm made from burnt brick clay 221x221x55 mm. All specimens were tested under axial compression. End conditions for each of the test specimen were kept similar. For the uniform distribution of load, rubber pads of 245x 245x6.125mm in size were placed at both ends of specimen and were covered with steel plates of dimensions 392x392x6.125mm. Ferrocement encased specimen was instrumented with strain gages at mid-height of the specimens. The parameters considered were mortar strength and thickness, spacing of reinforcement, bond between ferrocement casing and brick core on strength, width, and spacing of cracks. It was concluded that encasement of unreinforced brick masonry columns by ferrocement doubles the failure load and the average crack spacing reduces with reduction in spacing of wire.

In the present work, an experimental investigation on ferrocement-brick composite load bearing walls under axially concentrated compressive loads is carried out. These walls can be used as housing and rise building components.

Scope of the Work

In order to study the behaviour and ultimate strength of ferrocement encased brick walls when subjected to axial compressive load, a total of three ferrocement encased brick walls were built and tested. In addition, one brick wall with plaster only was built and tested under axial compressive loads.

All the models were of 1800 mm high×1000mm long×119mm wide and a total of 20mm ferrocement encasement thickness. The shape and dimensions of load-bearing walls built and tested in the present investigation are shown in Figure (1). The main parameter chosen was number of wire mesh layers (2, 3 and 4).

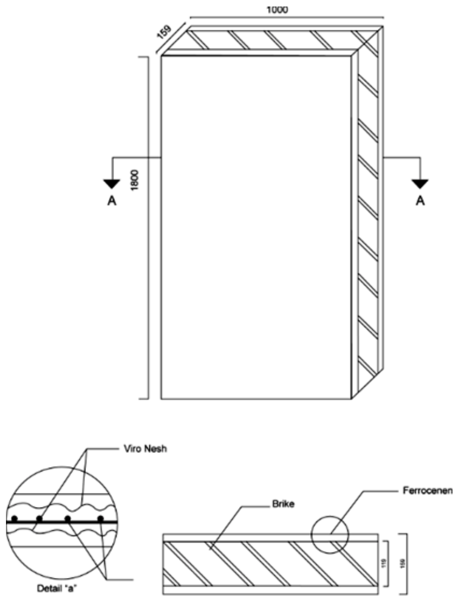

Figure1. *Dimensions and reinforcement arrangement of the tested wallsFiF*

Construction of Ferrocement-Brick Composite Walls

Brick Work

Brick

237×119×77mm solid bricks were used throughout. The compressive strength and water absorption tests were carried out and the average value of the compressive strength and water absorption for ten brick samples were found to be 12.5 N/mm^2 and 24% respectively.

Mortar

Mortar mix (sand: cement=3:1) and water/cement ratio of 0.7 were used. Compressive strength of mortar mixes were determined by testing three 100 mm cube for each wall as given in Table (1).

Table1. *Brick mortar compressive strength*

Wall No.	Compressive Strength (N/mm^2)
W1	26.4
W2	24.6
W3	27
W4	29.4

The walls were built by an experienced brick layers and cured using wet gunny bags spread over the surface and curing was continued until few days prior to casting the ferrocement casing.

Ferrocement Casing

Hexagonal wire mesh with skelatal smooth mild steel bar with an average diameters of 0.7mm and 5.5 mm respectively were used. Several strands of wires were taken from the mesh with samples of mild steel bar and tested in tension.

The average value of the yield stress (f_{my}), ultimate stress (f_{ult}), and the modulus of elasticity (E_s) calculated from the tests of wire meshes and mild steel bars are given in Table (2).

Table2. *Properties of wire mesh and skeletal reinforcement*

	Wire mesh 0.7 mm dia.	Smooth steel bar 5.5 mm dia.
Yield stress (f_{my})*, (N/mm^2)	300	510
Standard deviation	8.2	12.8
Ultimate Strength (f_{ult}), (N/mm^2)	520	582
Standard deviation	18.6	17.5
Modulus of elasticity (E_s) (N/mm^2)	6700	198820
Standard deviation	126	287

** The yield strength was selected as the stress corresponding to a total strain of 0.005.*

Ordinary Portland cement and sand passing through BS Sieve No.7 and conforming to Building Code Recommendations for Ferrocement (IFS 10-01)(4) were used throughout. The mix proportion of sand: cement used in casting the ferrocement casing was 2:1 by weight with water: cement ratio of 0.45.

After the brick works had been constructed, the mesh and skeletal reinforcement were cut to an appropriate size. The mesh layers were stretched, straightened and bounded to the skeletal reinforcement using mild steel binding wires. The skeletal reinforcements considered were 3 vertical bars (450 mm c/c) and 5-horizontal bars (425 mm c/c). considered (450 mm c/ars (425 mm c/c).

All the materials required were weighed carefully, and then mixed in a mechanical mixer. Sand and cement were first mixed for 1 min, then water was added and mixed for 2 min. The mortar was forced into the mesh reinforcement with trowels. Wooden flat plates were held in position on each side, so that the forced mortar could be confined with the required thickness.

Instrumentations

Demec type mechanical strain gauges of 200 mm length were used for measuring the strains. These strains were measured at several positions as shown in Figure 2(a).

The demec steel discs were fixed on the models using a bonding epoxy adhesive material. The lateral deflections were measured using dial gauges graduated in units of 0.01 mm. The positions of these dial gauges are shown in Figure 2(b).

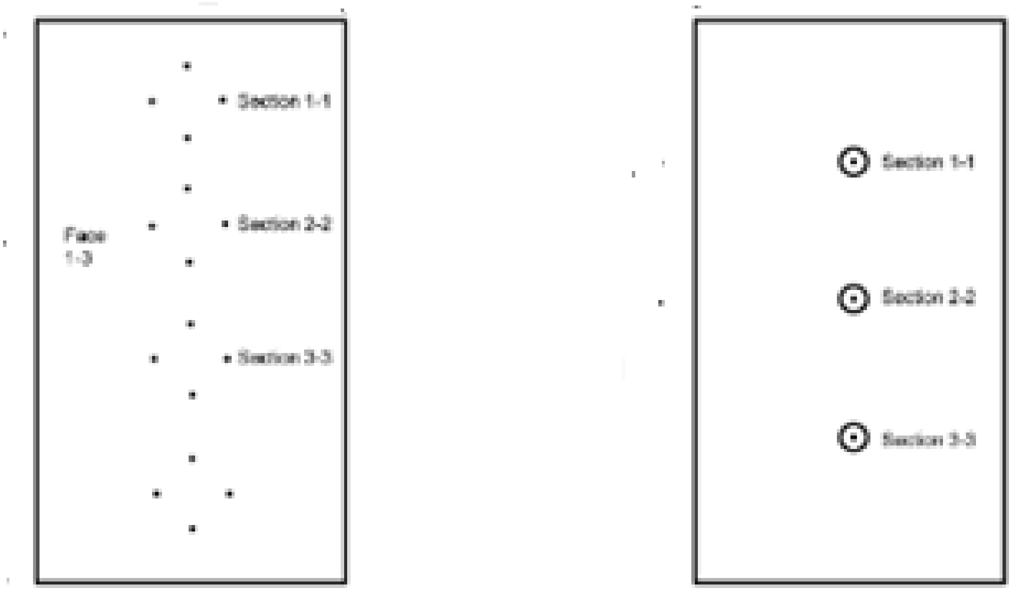

A. Positions of the demec B. Positions of the dial gauges

Figure2. *Positions of the instrumentations used through the investigation*

TESTING RIG

All models were tested in a 2450 kN capacity hydraulic Avery-type testing machine. Hinged end conditions were simulated using a flexible pad system as shown in Figure (3). Hence the effective height of load-bearing walls becomes the unsupported length of the model itself.

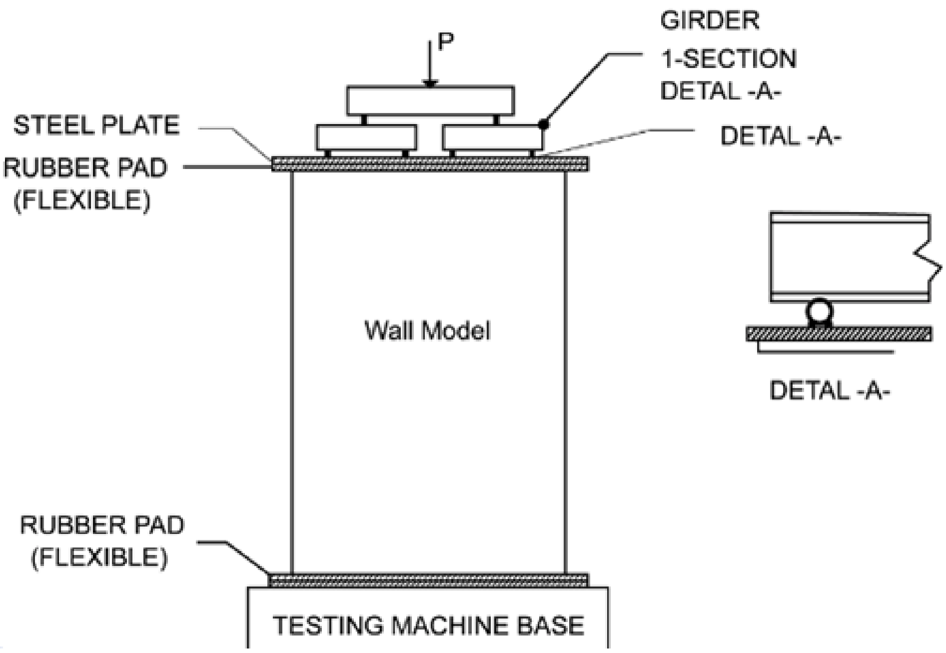

Figure3. *Testing rig*

TESTING PROGRAM

All models were painted white before testing so that cracks would be easily observed. Then, the steel discs for the mechanical strain gauges were fixed using bonding epoxy adhesive material, and the models were left for 24 hrs for the final setting of the adhesive material.

After the model was placed and accurately aligned in the testing machine, the rubber pads and steel plates were placed in position and the dial gauges were fixed at their appropriate locations.

The initial reading of the strain and dial gauges were recorded at the beginning of the tests, then the load was gradually applied in increment of 50 kN until failure occurred. The dial gauge readings were taken at least 2 min after each load increments to allow for the reading to become stable, and crack initiation was marked. The load application was continued until deformation became excessive. The models failed with cracking noise and spalling off the mortar cover over the meshes, associated with a rapid drop in the load response.

SUBSIDIARY TESTS

Since it was necessary to carry out test on each model, it was important to establish cube and cylinder mortar compressive strength (f_{cu}) and (f'_c), modulus of rupture (f_r), modulus of elasticity (E_m) and Poisson's ratio (□). Thus a number of control specimens were made, as given in Table (3). These tests were in accordance with BS 1881.

Table3. *Details of the control specimens*

Test type	Compressive strength		Modulus of Rupture, *fr*	Modulus of elasticity, Em and Poisson's ratio, v
	f'c	*fcu*		
Number and size of the specimens	Three 100x200 mm cylinders	Three 100 mm cube	Three 100x100x400 mm prisms	Three 150x300 mm cylinders

Test samples were taken directly from the material used for the construction of models. Curing condition of test samples and models were the same. The results of the control specimens tested are given in Table (4).

Table4. *Test results of control specimens.*

Wall No.	Mortar 1:2 cement : sand				
	Compressive strength (N/mm^2)		Modulus of rupture, fr (N/mm^2)	Modulus of elasticity, Em (N/mm^2)	Possion's ratio, ν
	f'_c	f_{cu}			
W1	39.55	40.12	2.8	27562	0.24
W2	39.9	42	2.81	27956	0.236
W3	39.32	42.5	2.85	27836	0.234
W4	36.42	40.65	2.83	27230	0.2
Av.	38.79	41.31	2.82	27646	0.2275

In order to determine the characteristic compressive of brick masonry (f_k)for each model, prisms tests rather than tests of single brick to determine the compressive strength was adopted because the standard brick compressive test does not correlate well with that of the brick-mortar assemblage(5). The prisms were made from the same materials with the same bonding arrangements as those of the models. The moisture content and consistency at the time of laying as well as the mortar joint thickness should approximate the actual model conditions as closely as possible.

Test prisms should be one masonry unit in plane for a height to depth (h/d) ratio of about 1-2. The results of the prisms tested to establish the design strength of brick masonry (f_k) are given in Table (5).

Table5. *Values of compressive strength of the tested prisms*

Wall No.	f_k (N/mm^2)
W1	5.4
W2	5.31
W3	5.32
W4	5.43

The compressive strength of brick unit measured experimentally is equal to 12.5 N/mm^2, therefore the characteristic compressive strength (f_k) is 5.2 N/mm^2 as given in Table (6).

Table6. *Characteristic compressive strength of masonry, fk (N/mm2) (BS. 5628: Part 1)*

Mortar Designation	Compressive Strength of Bricks (N/mm^2)								
	5	10	15	20	27.5	35	50	70	100
i	2.5	4.4	6.0	7.4	9.2	11.4	15.0	19.2	24.0

i for sand : cement = 3:1

This value is seen to be in a very good agreement with those measured experimentally as given in Table (5).

RESULTS

Table (7) gives the observed cracking load, ultimate load, and mode of failure of each ferrocement-brick composite wall.

In general, at the early loading stage it was observed that the models behaved elastically until the first crack appeared. It was started with a longitudinal crack along the loading direction. It may be noticed from Table (7), that the cracking loads range between (30-40%) of the ultimate loads.

Table7. *Measured values of the tested walls*

Wall Mark	No.of Wire Mesh Layers	Initial Cracking Load (kN)	Ultimate Load (kN)	Mode of Failure
W1	4	300	801	All walls failed with spalling of the mortar cover over the mesh with longitudinal cracking along the loading direction at the top and the bottom
W2	3	310	840	
W3	2	250	825	
W4	-	200	377	Large cracking along the loading direction

A typical stress-strain curve in longitudinal direction is shown in Figure (4).

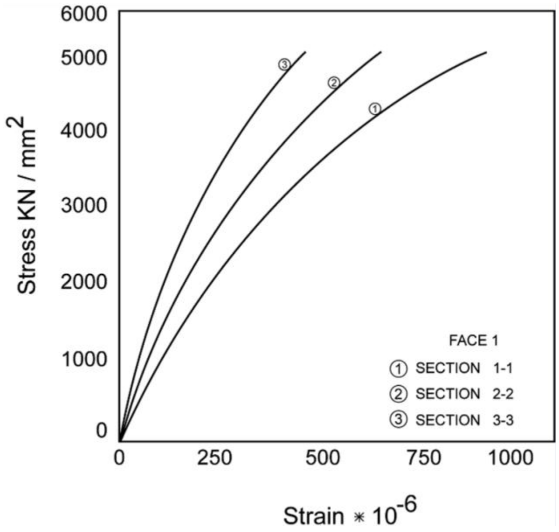

Figure4. *A typical stress-strain curve in the longitudinal direction*

It was observed that strain values in the transverse directions were nearly equal to zero up to 60% of the ultimate strength. The observed cracks are longitudinal cracks along the loading direction of the tested walls. The first crack was observed at the top end of the walls. The cracks were increased by increasing the load. It was observed that increasing the number of wire mesh layers tends to increase the number of cracks and decrease the cracks spacing. Ferrocement casing do not show any appreciable spalling or splitting leading to separation of mortarfromthe mesh at working loads.Lateral deflections are recorded for different stages of loading and plotted in Figure (5).

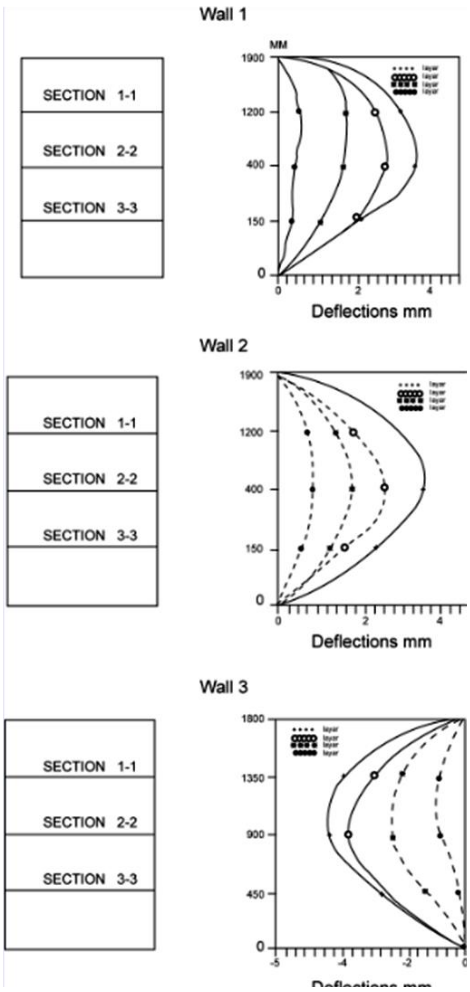

Figure5. *Lateral deflections along the wall height*

The lateral deflections are too small (1-4 mm) which can be ignored in the analytical solution.

Design of Brick - Ferrocement Composite

It is assumed that the strength of brick-ferrocement composite wall can be determined by simply adding the brick strength component to the ferrocement component. In simple terms, ultimate load P_u is given by the following expression:

$$P_u = P_1 + P_2 \quad (1)$$

where:

P_1 : load carrying capacity of brick wall.

P_2 : load carrying capacity of ferrocement casing.

Brick Wall Strength (P1)

The load carrying capacity of brick wall is based on the procedure given by Andrew Ortan[6] and Structural Masonry Designer's Manual[7], as follows:

The design of load carrying capacity of a brick wall per unit length is given by:

$$P_1 = \square .t.f_k \quad (2)$$

where:

□□: capacity reduction factor obtained from Table (8).

Table8. *Capacity reduction factor, β (BS.5628: Part 1)*

Slenderness Ratio, h_{ef} / t_{ef}		**0**	**6**	**8**	**10**	**12**	**14**	**16**	**18**	**20**	**22**	**24**	**26**	**27**
Eccentricity at top of wall, ex	Up to 0.05 t*	1.0	1.0	1.0	0.97	0.93	0.89	0.83	0.77	0.7	0.62	0.53	0.45	0.4

** It is not necessary to consider the effects of eccentricities up to and including 0.05t.*

f_k : characteristic compressive strength of the masonry obtained from Table (6).

t: thickness of the wall.

If the horizontal cross-section area of a loaded wall is less than 0.2 m^2, the characteristic compressive strength should be multiplied by the factor (0.7+1.5 A_b), where A_b is the horizontal loaded cross sectional area of the wall (m^2).

The slenderness ratio should not exceed 27, except in the case of wall with less than 90 mm thick, it should not exceed 20.

The effective height of a wall is taken as the clear distance between lateral movements.

Ferrocement Casing Strength (P2)

For the evaluation of ultimate compressive load of ferrocement bearing wall element, the following expressions are considered [8,9]:

a) $$P_2 = K f_{cu} + f_{my} A_m \quad (3)$$

It is assumed that steel bars used in the wall element serve to tie the meshes together and do not carry any load.

b) $$P_2 = K f_{cu} + f_{my} A_m + f_{sy} A_s \quad (4)$$

The steel bars are assumed to be stressed to their yield stress and this could be possible if they get enough lateral support from the meshes embedded in mortar.

c) $$P_2 = f_r A_g \quad (5)$$

In equation (5) any contribution from skeletal bar reinforcement towards carrying the load is neglected.

d) $$P_2 = f_f A_g + f_{sy} A_s \quad (6)$$

Equation (5) is modified to include the influence of steel bars that are assumed to yield at ultimate.

e) $$P_2 = 0.55\ \square\ f_c\ A_g [1-(Le/40h)^2] \quad (7)$$

Ultimate load is determined according to the relation given by ACI-318-71 for reinforced concrete wall elements, interpreted to suit the ferrocement wall element.

f) The ultimate load calculated using the relation for short braced axially loaded reinforced concrete walls given in CP:110[10] is modified to include the area of wire mesh in the direction of loading.

$$P_2 = 0.4 f_{cu} A_c + 0.67 (A_m f_{my} + A_s f_y) \quad (8)$$

g) $$P_2 = 0.67 f_{cu} A_g [1-(Le/40h)^2] + 0.67(A_m f_{my} + A_s f_y) \quad (9)$$

where;

P_2 : load carrying capacity of ferrocement.

A_c : area of mortar in ferrocement element.

A_g : gross cross section area of element.

A_m : area of wire mesh in loading direction.

A_s : area of steel bar reinforcement.

f_{cu} : cube strength of mortar.

f'_c : compressive strength taken equal to f_{cu} in case of mortar when applied to ferrocement element.

f_f : compressive strength of 300×150×20mm ferrocement plate (taken as 83% of cube strength of mortar).

f_{my} : yield strength of wire mesh.

f_{sy} : yield strength of bar reinforcement.

H : overall thickness of ferrocement wall element.

K : reduction factor = 0.7

L : length of ferrocement wall element.

L_e : effective height, equal to length of ferrocement wall element.

□□: capacity reduction factor = 0.7.

These expressions take into account the influence of L/h ratio and the contributions from mesh and bar reinforcement.

The values of ultimate load calculated using expression (1) are tabulated in Table (9).

Table9. *Comparison of the computed ultimate loads with the measured values*

Wall No.	Pex (kN)	P_1(kN) Equ.2	P2(kN) Equ.3	Pex Pu	P2(kN) Equ.4	Pex Pu	P2(kN) Equ.5	Pex Pu	P2(kN) Equ.6	Pex Pu	P2(kN) Equ.7	Pex Pu	P2(kN) Equ.8	Pex Pu	P2(kN) Equ.9	Pex Pu
W1	801	412.2	994.1	0.57	1066	0.54	1199	0.49	1271.4	0.47	554.6	0.82	633	0.75	1009	0.64
W2	840	412.2	1007.3	0.6	1080	0.56	1255	0.5	1327.5	0.48	580.6	0.84	653	0.78	1086	0.56
W3	825	412.2	975.3	0.59	1048	0.56	1215	0.5	1287.5	0.48	587.5	0.82	646.1	0.78	1089	0.54

It is seen that expression (7) gives better predication to the ultimate load.

Summing the forces in the composite section and dividing through by A_t and ∈ yields,

$$E_t = E_f \,.\, a_f + E_b \,.\, a_b \qquad (10)$$

where;

E_t : modulus of elasticity of ferrocement-brick composite.

E_f : modulus of elasticity of ferrocement composite.

E_b : modulus of elasticity of brick core = 350 $\sqrt{f_k}$

a_f: ratio of ferrocement cross sectional area to the composite cross-sectional area.

a_b: ratio of brick cross sectional area to the composite cross-sectional area.

To determine the modulus of elasticity of the ferrocement composite (E_f), 18 (9x2) ferrocement hollow cylinders 300×150×20mm were cast and tested under axially compressive load. The hollow cylinders were reinforced with 2, 3 and 4 wire mesh layers and sand: cement ratio of (3:1), (2:1) and (1:1). Full details of these hollow cylinders are given in Table (10).

Table10. *Details of ferrocement hollow cylinders.*

Ferrocement H.C No.	Dimension (mm)	Cement to Sand ratio	No. of wire mesh layers
1,2	300x150x20	1:3	4
3,4	300x150x20	1:3	3
5,6	300x150x20	1:3	2
7,8	300x150x20	1:2	4
9,10	300x150x20	1:2	3
11,12	300x150x20	1:2	2
13,14	300x150x20	1:1	4
15,16	300x150x20	1:1	3
17,18	300x150x20	1:1	2

For a typical repeating section of the hexagonal mesh, the longitudinal specific surface of each ferrocement hollow cylinder (S_L) was calculated and tabulated in Table (11).

Table11. *Specific surface and composite modulus of elasticityof ferrocement hollow cylinders.*

Ferrocement H.C No.	**1**	**2**	**3**	**4**	**5**	**6**	**7**	**8**	**9**
S_L (l/mm)	0.033	0.0247	0.0165	0.033	0.0247	0.0165	0.033	0.0247	0.0165
E_f exp. (N/mm^2)	19740	18450	17220	28142	26608	25480	32210	28560	27816
E_f eq.(11) (N/mm^2)	21145	19539	17952	26313	24707	23119	32092	30485	28898
E_f exp./E_f pro.	0.93	0.94	0.96	1.07	1.07	1.1	1.00	0.94	0.96

The test results of ferrocement hollow cylinder are given in Table (12) and a typical stress-strain curve is shown in Figure (6).

Table12. *Ferrocement hollow cylinder test results.*

Hollow Cylinder No.	**Cement to sand Ratio**	**No. of wire Mesh layers**	**Cub strength, f_{cu} (N/mm^2)**	**Compossive strength of ferrocement, ff (N/mm^2)**	**Composite modulus of elasticity, E_f (N/mm^2)**
1	1:3	4		23.55	19740
2	1:3	3	29.6	24.55	18450
3	1:3	2		22.73	17220
4	1:2	4		29.87	28142
5	1:2	3	43.3	34.27	26608
6	1:2	2		33.6	25480
7	1:1	4		51.41	32210
8	1:1	3	61.7	56.31	28560
9	1:1	2		52.8	27818

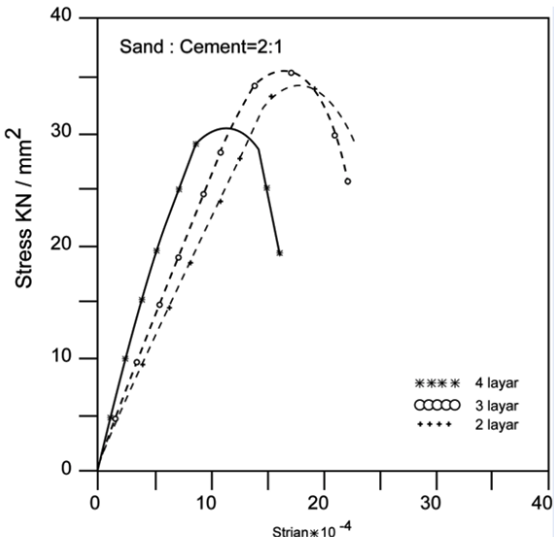

Figure6. *Stress-strain curve of ferrocement hollow cylinder*

From stress-strain curves and compressive strength of ferrocement (f_f), the composite modulus of elasticity of ferrocement (E_f) is established as given in Table (11).

For the design purpose, the strain □ in the longitudinal direction of ferrocement-brick composite is assumed to be equal to 0.0006, therefore, the following expression for the determination of ultimate load is proposed:

By using regression analysis, the following expression to predict the ferrocement composite modulus of elasticity is proposed and the values are tabulated in Table (12):

$$P_u=(2.72\sqrt{f_{cu}}+116.129S-5.945)\ A_f + 0.21\sqrt{f_k}\ A_b \quad (12)$$

The comparison between the values of ultimate load using the proposed expression with the measured values is tabulated in Table (13).

Table13. *Comparison of the computed ultimate loads using the proposed expression (12) with the measured values.*

Wall No.	**$P_{exp.}$**	**$P_{u(prop.)}$**	**P_{exp} / P_u**
W1	801	952	0.84
W2	840	862	0.97
W3	825	793	1.04

Allowable Load and Design Factor of Safety

The allowable load can be determined simply by adding the allowable load of ferrocement casing to brick core.

Ferrocement Casing

The allowable load of ferrocement casing is[7]:

$$P_{all.} = 0.2\, f'_c\, [1-(h/40t_c)^3]\, A_g \qquad (13)$$

where;

f'_c : compressive strength taken equal to f_{cu} in case of mortar when applied to ferrocement elements.

H : hight of ferrocement casing.

t_c : overall thickness of ferrocement casing.

A_g : gross cross sectional area of casing.

Brick Core

The allowable load of brick core is[4]:

$$P_{all.} = 0.2\, f_k\, [1-(h/42t_b)^3]\, A_b \qquad (14)$$

where;

h : height of brick core.

t_b : thickness of brick core.

Thus the allowable load of ferrocement composite wall is:

$$P_{all.} = 0.2\, [f'_c\, (1-(h/40\, t_c)^3)A_g + f_k\, [1-(h/t_b)^3\, A_b] \qquad (15)$$

and design factor of safety is:

$$\gamma = P_u / P_{all.} \qquad (16)$$

The values of allowable load of ferrocement composite walls and design factor of safety are tabulated in Table (14).

Table14. *Values of calculated ultimate load, allowable load, Pall. and factor of safety γ*

Wall No.	Pex.(kN)	Allowable load Pall.(kN)	Factor of safety γ
W1	952	444.6	2.14
W2	862	459.7	1.875
W3	793	463.7	1.710

Conclusions

This investigation has shown that ferrocement-brick composite can be satisfactorily used as a compression element. The high load carrying capacity of the ferrocement-brick composite makes it feasible to be used as housing components and for rise buildings with adequate structural safety. It may also be concluded that ferrocement casing leads to have a ductile failure compared to brittle failure of a brick wall coated with mortar.

References

[1] K. K. Singh, S.K. Kaushik and Anand Prakash. "Strengthening of Brick Masonry Columns by Ferrocement". Ferrocement; Applications and Progress. Proceeding of the Third International Symposium On Ferrocement,University of Roorkyee, Roorkee, India 8-10 December, 1988 PP 306-313.

[2] G. C. Nayak and S. C. Jain. "Tests on Composite Masonry Ferrocement Elements". Ferrocement; Applications and Progress. Proceeding of the Third International Symposium On Ferrocement,University of Roorkyee, Roorkee, India 8-10 December, 1988 PP 375-385.

[3] Al-Rifaie W.N., and Mohammad K.A., "The Strength of Ferrocement-Brick Composite Columns", Journal of Ferrocement, Vol. 30, No. 1, January 2000, PP.69-83.

[4] Ferrocement Model Code, Building Code Recommendations for Ferrocement, IFS 10-01, International Ferrocement Society, Asian Institute of Technology, Bangkok, Thailand, January 2001.

[5] Robert, R. Schneider and Walter, L. Dickey "Reinforced Masonry Design", Prentice-Hall, Inc., Englewood Cliffs, NewJersey, 1987.

[6] Andrew Orton, "Structural Design of Masonry" Longman, London and New York, 1986.

[7] Curtin, W.G., Shaw G., Beck J.K. and Bray W.A., "Structural Masonry Designer's Manual", Second Edition, BSP Professional Books, 1987.

[8] Desayi, P., and Kumar. G.R.P., "Ferrocement Load Bearing Wall Element", Journal of Structural Division, ASCE, Sept., 1976, pp.1903-1916.

[9] Desayi, P., and Kumar. G.R.P., "Lightweight Ferrocement Wall Element", Journal of Ferrocement, Vol.7, No.1, July 1977, pp.28-36.

[10] British Standards. Code of Practice for Structural Concrete CP110, Part 1, Design materials and Workmanship. 1972.

Citation: *W. Al-Rifaie and K. Mohammad, "Load Carrying Capacity of Clay Brick Masonry Wall Encased by Ferrocement", International Journal of Emerging Engineering Research and Technology, vol. 5, no. 4, pp. 26-35, 2017.*